

Athermalization of a type of fisheye optical system in the temperature range of Iran

Yasin Zakerinasab , Ali Rezaei-Latifi* 

Department of Physics, Faculty of Sciences, University of Hormozgan, Bandar Abbas, Iran.

*Corresponding author: r_latifi@hormozgan.ac.ir

Original Research

Abstract:

Received:
8 March 2024
Revised:
22 July 2024
Accepted:
26 July 2024
Published online:
30 August 2024

The fisheye system belongs to the family of ultra-wide field of view lenses and has various applications in science, industry, surveillance and artistic fields. Such lenses can cover a field of view of 180 degrees or even larger in the shape of a hemisphere, and therefore can provide the possibility of imaging a large part of the surrounding space with just one shot. Due to the wide temperature changes in Iran, the optical performance of this system is significantly reduced under the influence of the change in the radius and thickness of the surfaces and the change in the refractive index of its glasses. Therefore, in order to achieve optical-thermal stability in the temperature range of Iran, it is necessary to athermalize the system so that temperature changes do not cause a noticeable decrease in the optical performance of the system. In this work, a type of fisheye optical system is redesigned in the visible light spectrum bandwidth and then it is athermalized in the temperature range of Iran from -46 to 70 degrees Celsius.

© The Author(s) 2024

Keywords: Fisheye lens; Athermalization; Distortion aberration; Spot diagram; Strehl ratio; Modulation transfer function

1. Introduction

Athermalization in the field of optics is the process of achieving optothermal stability in optomechanical systems [1, 2]. The optical materials of imaging systems expand and contract in response to temperature changes, which causes changes in the radius of the surfaces, the shape of the surfaces and the thickness between them. The change in material dimensions is described by a quantity called thermal expansion coefficient. In optomechanical systems, in addition to the change in the dimensions of the glass elements, the expansion and contraction in the lens housing also changes the optical performance. Also, temperature changes cause a change in the refractive index of optical materials, which causes defocusing and reducing the optical performance of the system [3, 4]. In the athermalization process, with techniques such as using suitable glass elements and changing the radius and thickness of the surfaces and using a suitable lenses housing, the changes in optical performance in a wide range of temperatures are minimized. The fisheye lens is a bionic system that mimics the eyes of underwater fish, which look at the upper half of the seawater. A fish immersed in water takes its eyes directly to

the surface of the water and sees objects above the surface as a compressed circular image with a field of view of approximately 180 degrees, although the image is strongly distorted at the edge. By designing the function of a fish eye as an optical tool, a fish-eye lens is obtained [5, 6]. Since the first fisheye lens, the "Hill Sky lens" [7] was introduced in 1924, fisheye lenses have been in development for almost a century. The history of a simple fisheye simulation can even be traced back to the first fisheye pinhole camera made by Wood in 1906 [8]. A number of excellent fish-eye lenses have been designed in the past decades, and the designs have improved especially in image quality [9–12]. Despite the relatively significant development of fisheye lenses in the last century, there are not many sources other than patents on the subject of fisheye lens design. Even in standard lens design books [13–15], the fisheye lens topics were only mentioned in a few sentences while other lens design topics were discussed in detail.

Although the primary purpose of fisheye lenses was to record clouds in the sky, today they are used in various fields of engineering, defense, surveillance and art. Fish-eye lenses are widely used in creative photography, dome film projection in planetariums, meteorological monitoring,

safety monitoring, positioning of celestial objects, engineering measurement and micro-intelligent systems [16, 17].

Due to the wide seasonal and spatial temperature changes in Iran, the performance of optomechanical instruments decreases under the influence of temperature changes. Because optical instruments are usually designed and optimized at a specific temperature, therefore, the optical performance decreases with increasing or decreasing temperature. In this paper, a type of fisheye lens, which was previously designed to create a good quality image at a temperature of 20 degrees Celsius, is athermalized for optical stability in the temperature conditions of Iran. In the following, at first, the materials and method of athermalization are described, and then the results of the athermalization of the system are discussed.

2. Materials and methods of athermalization of the system

2.1 Fisheye lens

Fisheye lens systems are usually optical systems consisting of a front group and a rear group. Front group lenses usually consist of negative meniscus lenses with a larger absolute focal power. The first lens in the front group, in particular, has a much larger negative focal power and is a telephoto objective lens. The rear group has positive focal power. The main work of the front group of fisheye lenses is to compress the angle of the field of view after the incident light passes through the front group, which is beneficial for designing the rear group and correcting the aberration of the whole system [12]. The fisheye lens that is athermalized in this work was designed by Guozhu and Lijun, [12]. In this design, the front group includes 5 lenses, the power of the fourth lens is positive and the power of the rest is negative. The rear lens of the system consists of 9 lenses, and both of the adjacent lenses are attached from lenses 7 to 10 and lenses 12 to 13. The power of the 6th, 11th and 14th lenses is negative and the power of the other lenses is positive. The specifications of this system, including the type of lenses, the radii of curvature and the thickness of the surfaces, have been presented in the paper of Guozhu and Lijun [12].

2.2 The effect of temperature on focal length and optical performance

We consider a thin lens with refractive index n , focal length f , and power φ at temperature T . The lens power is obtained from the following equation [18, 19]:

$$\varphi = (n - 1)(C_1 - C_2) \quad (1)$$

where C_1 and C_2 are the curvature of the front and back surfaces of the lens. The curvature of the surface is the inverse of the radius of surface R .

Derivation of the above relation with respect to temperature gives:

$$\frac{d\varphi}{dT} = \frac{dn}{dT}(C_1 - C_2) + \left(\frac{dC_1}{dT} - \frac{dC_2}{dT}\right)(n - 1) \quad (2)$$

On the other hand:

$$\frac{dC_1}{dT} = \frac{d(1/R_1)}{dT} = -\frac{1}{R_1^2} \times \frac{dR_1}{dT} \quad (3)$$

$$\frac{dC_2}{dT} = \frac{d(1/R_2)}{dT} = -\frac{1}{R_2^2} \times \frac{dR_2}{dT} \quad (4)$$

but we have:

$$\frac{1}{R_1} \frac{dR_1}{dT} = \frac{1}{R_2} \frac{dR_2}{dT} = \alpha \quad (5)$$

where α is the thermal expansion coefficient of the lens. So we will have:

$$\frac{d\varphi}{dT} = \varphi \left[\frac{\frac{dn}{dT}}{n-1} - \alpha \right] \quad (6)$$

$$\frac{d\varphi}{dT} = -\frac{1}{f^2} \frac{df}{dT} \quad (7)$$

As a result, we get [20]:

$$\frac{df}{dT} = -f \left[\frac{\frac{dn}{dT}}{n-1} - \alpha \right] \quad (8)$$

which can be written as the following formula:

$$\Delta f = -\left(\frac{\frac{dn}{dT}}{n-1} - \alpha \right) f \Delta T = -\gamma f \Delta T \quad (9)$$

in which the thermo-optic coefficient of the lens is defined as follows:

$$\gamma = \left(\frac{\frac{dn}{dT}}{n-1} - \alpha \right) \quad (10)$$

2.3 The effect of temperature on the lens housing

Thermal defocus is not only from the change of optical power of the lens, but also from the coefficient of thermal expansion of the housing α_h . Equation (8) can be modified as follows to take this effect into account [20, 21]:

$$\Delta f = -f(\gamma + \alpha_h)\Delta T \quad (11)$$

The effect of temperature change on the length change of the lens housing is determined from the following equation:

$$\Delta L_h = L_h \alpha_h \Delta T \quad (12)$$

where ΔL_h is the length change of the housing, L_h is its initial length and ΔT is the temperature change. In this research, the material of the housing aluminum with a thermal expansion coefficient of $23 \times 10^{-6} 1/^\circ\text{C}$ is chosen due to its good flexibility, light weight and reasonable price [22].

According to the above formulas, for j thin lenses in contact with the effective focal length f , we obtain the change in focal length due to the change in temperature ΔT as follow:

$$\Delta f = -f^2 \sum_{i=1}^j (\gamma_i \varphi_i + \alpha_h) \Delta T \quad (13)$$

2.4 Input data and system optimization and athermalization method

As mentioned in section 2.1, the data of the paper of Guozhu and Lijun [12] were used for the initial design of the fish-eye lens. Zemax software was used for redesigning and thermalization. After inputting the lens data, a fisheye system was redesigned with the specifications listed in Table 1. Then,

Table 1. Basic specifications of fisheye lens.

parameter	Value
Image space F-Number	3.60
Image space NA	0.14
Effective focal length	7.82 mm
Back focal length	17.17 mm
Field of view	180°
Entrance pupil diameter	2.17 mm
Exit pupil diameter	20.51 mm
Wavelength	486 – 656 nm

according to the temperature range of Iran, temperature changes were applied from -46 to 70 degrees Celsius. The temperature of about 70 degrees is the highest temperature recorded in the Iran country, which is related to Lut plain in Kerman provinc. In 2004 and 2005, Iran's Lut desert was the Earth's hottest spot [23]. Also, the northwestern regions are the coldest regions of Iran [24]. According to the report of the Meteorological Organization of the Islamic Republic of Iran, the temperature of -46 degrees was recorded in the city of Saqqez along with the city of Bostan Abad in East Azarbaijan province, and they have been called the coldest cities in Iran.

In the process of athermalization, it is tried to bring the root mean square radius (RMS radius) of the spot diagram to a minimum value at different temperatures. The RMS radius is obtained from the following equation:

$$\text{RMS} = \sqrt{\frac{\sum_i [(x_i - x_c)^2 + (y_i - y_c)^2]}{n}} \quad (14)$$

which in the above formula (x_c, y_c) are the coordinates of the chief ray and (x_i, y_i) are the coordinates of other rays on the image plane, all of which are emitted from the same point of the object, and n is the number of selected rays. When all the emitted rays meet at the location of the chief

ray, then the RMS radius is zero, which means that the aberration of the image of that point from the object is zero. But in practice, there are always aberrations, and the larger the RMS radius of the spot diagram, the larger the aberrations will be. In the optimization process, by changing the radius and thickness of the surfaces and the type of glass and defining a function called the merit function, we will try to reduce the value of the RMS radius to the minimum value. The merit function, MF, is defined as follows:

$$(\text{MF})^2 = \frac{\sum_i W_i (V_i - T_i)^2}{\sum_i W_i} \quad (15)$$

In the above equation, T_i is the target value and V_i is the current value of operands defined in the merit function editor of Zemax software, w_i and is the weight of each operand. In this design, TRAC operands are used for optimization, the value of this operand is the distance between the coordinates of the selected ray compared to the chief ray. Because the goal of optimization is to bring the value of this operand close to zero, we consider its target value to be zero. In optimization, the current value of this operand for each ray before optimization is tried to approach its target value, i.e. to zero value after optimization. In the process of athermalization, optimization is done in the temperature range of Iran, i.e. from -46 to 70 degrees Celsius.

3. Results

Figure 1 shows the designed fisheye lens after athermalization. As the figure shows, the rays entering the lens are well focused on the image plane at the field angle of zero to 180 degrees. The parameters that determine the quality of the image such as spot diagram, modulation transfer function (MTF) and Strehl ratio show that the designed system is well athermalized in the temperature range of Iran. After the athermalization of the system in the temperature conditions of Iran, some data of system lens designed by Guozhu and Lijun [12] were changed. Table 2 shows the system lens data after athermalization.

Figures 2 to 5 show the spot diagram at temperatures of -46 and 70 degrees Celsius respectively at a field angle of

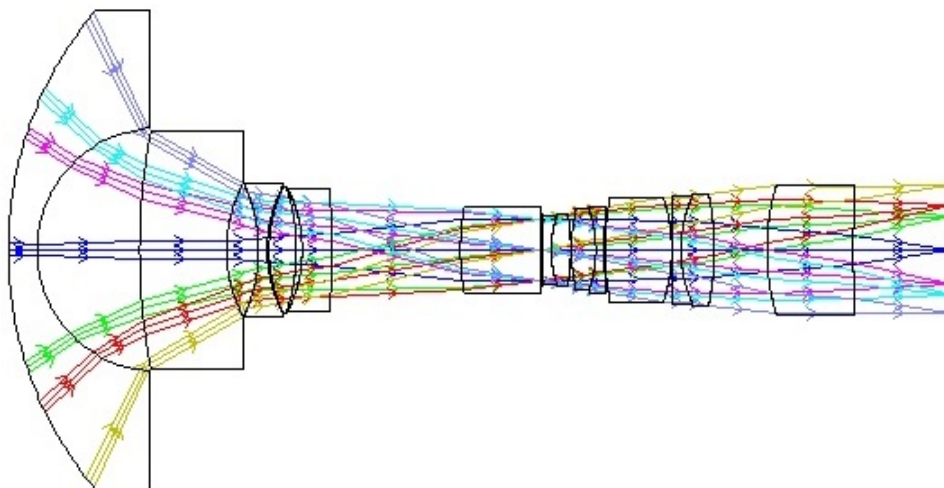


Figure 1. The three-dimensional layout of athermalized fisheye system in the temperature range of Iran.

Table 2. Data of athermalized fisheye lens at 20 degrees.

Surface	Surface type	Radius (mm)	Thickness (mm)	Glass	Semi-Diameter	TCE (10^{-6})
Object	Infinity	Infinity	Infinity	-	Infinity	0
1	Standard	64.804	4.998	LAH 66	41.576	-
2	Standard	21.233	17.837	-	21.157	0
3	Standard	111.285	15.090	N-LASF31A	20.764	-
4	Standard	24.392	5.573	-	11.624	0
5	Standard	-27.431	1.499	N-PSK57	11.719	-
6	Standard	24.064	0.340	-	11.004	0
7	Standard	26.042	4.737	PBH6W	11.021	-
8	Standard	-34.067	0.999	-	10.958	0
9	Standard	-24.281	5.206	LASFN31	10.751	-
10	Standard	-114.116	22.288	-	10.583	23
11	Standard	41.987	13.877	NLASF41	7.583	-
12	Standard	2917.865	0.310	-	5.563	0
13	Standard	Infinity	0.101	-	5.474	0
14	Standard	166.046	1.499	N-LASF31A	5.532	-
15	Standard	18.643	3.386	NSL3	5.852	-
16	Standard	-37.689	0.099	-	6.353	0
17	Standard	29.222	4.264	BK3	6.804	-
18	Standard	-21.075	1.499	N-LASF31A	7.060	-
19	Standard	147.630	0.1	-	7.533	0
20	Standard	45.415	11.609	TIFN5	7.747	0
21	Standard	-28.890	0.099	-	9.174	0
22	Standard	339.067	1.499	N-LASF40	9.242	-
23	Standard	22.797	5.802	N-PK52A	9.375	-
24	Standard	-46.164	9.138	-	9.797	23
25	Standard	39.657	14.991	S-FSL5Y	11.255	-
26	Standard	174.317	17.140		11.029	23
Image	Standard	Infinity	-	11.228		0

60 and 90 degrees for the spectral line d (yellow light with a wavelength of 587 nm) which is almost in the middle of the visible spectral region. For all three temperatures, almost all the points are located inside the Airy disc and the RMS radius of the point diagram is smaller than the Airy disc radius. The Airy disc is actually the smallest point where the rays emitted from a point of an object can be focused in the presence of the diffraction phenomenon in the absence of any type of aberration. Our research showed that in most of the lower half angle of the field i.e. between 0 and 90 degrees and the upper half angle i.e. between -90 and 0 degrees, most of the points (except for a few) are located inside the Airy disc, which indicates good image quality. It is at a temperature between -46 and 70 degrees Celsius. Figure 6 shows the diagram of the RMS radius against the

lower half angle of the field for the spectral line d at the temperature of -46 degrees Celsius. As this diagram shows, the RMS radius is smaller than the diffraction limit (Airy disc radius) in all field angles except in the range of 71 to 84 degrees. The main reason for that is the presence of high distortion aberration in larger field angles. The diagram for the upper half angle is almost the same.

Figures 7 to 10 describe the MTF modulation transfer function for temperatures of -46, 20 and 70 °C respectively at a field angle of 60° and for temperature of -46 at the field angle of 90° as a function of spatial frequency for spectral line C (red light with a wavelength of 656 nm) and d. In the ideal optical system, the wavefront emitted from the object is transmitted without any deviation. But in any real optical system there is a limit to the aperture, and the aperture

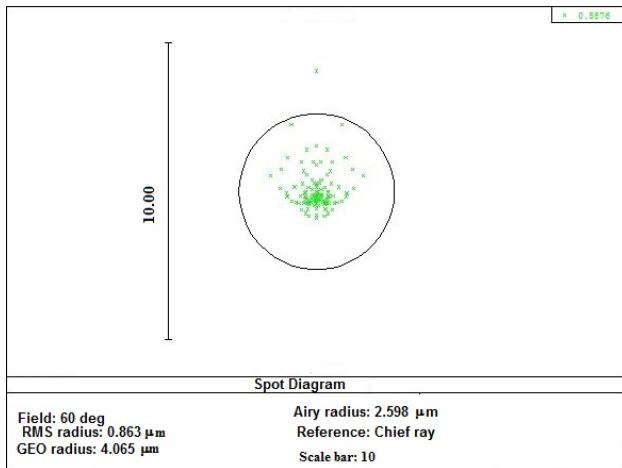


Figure 2. Spot diagram in wavelength of d at -46°C temperature for field angle of 60° .

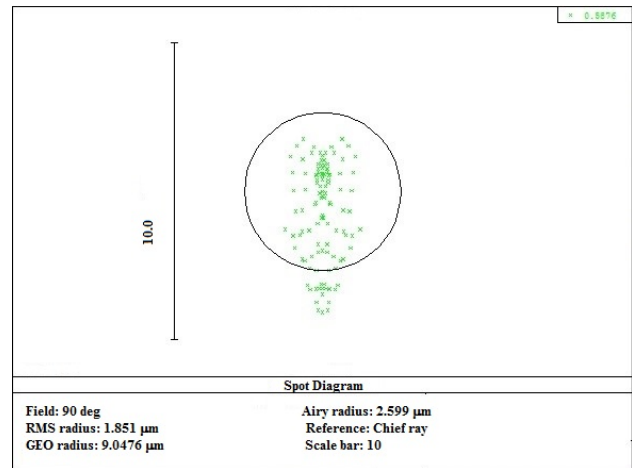


Figure 5. Spot diagram in wavelength of d at 70°C temperature for field angle of 90° .

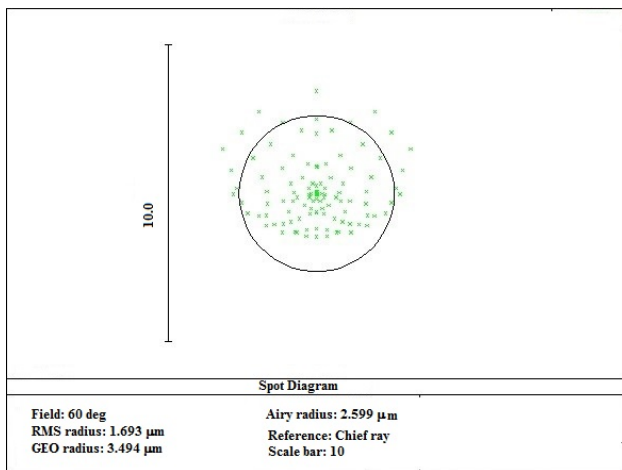


Figure 3. Spot diagram in wavelength of d at 70°C temperature for field angle of 60° .

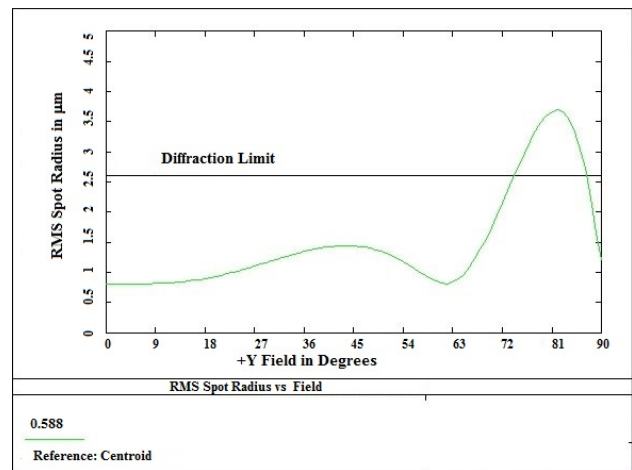


Figure 6. RMS radius of the diagram spot versus field in wavelength of d at a temperature of -46°C .

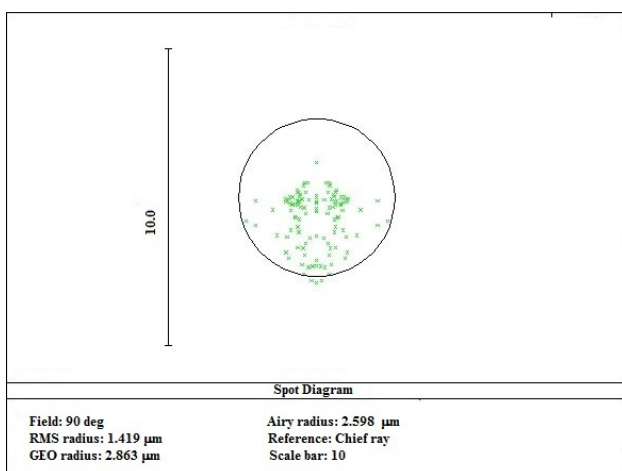


Figure 4. Spot diagram in wavelength of d at -46°C temperature for field angle of 90° .

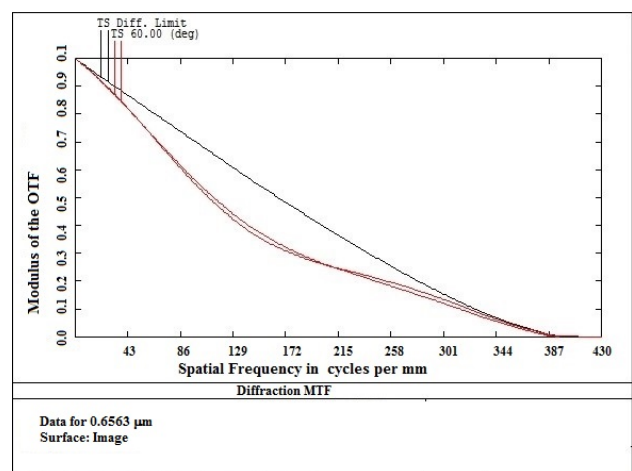


Figure 7. MTF diagram at -46°C temperature at 60° field angle in wavelength of d .

causes diffraction which lowers the MTF. In this diagram, the x -axis is the spatial frequency in units of line pairs per millimeter, and the y -axis is the absolute value of the phase

transfer function (contrast). A human generally needs a contrast of 0.1 or higher to be able to see the difference between lines. The black curve is the diffraction limit dia-

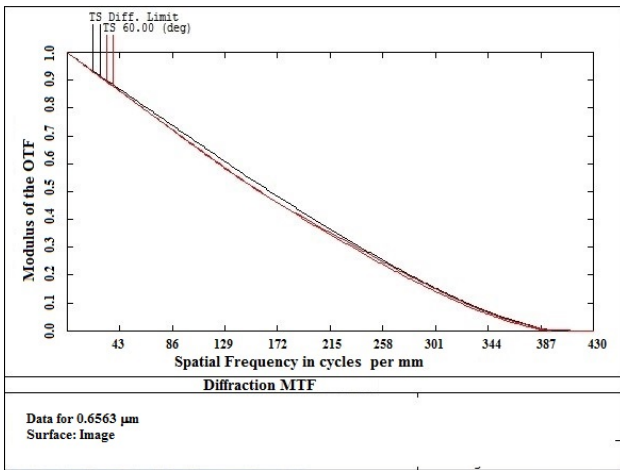


Figure 8. MTF diagram at 20 °C temperature at 60° field angle in wavelength of C.

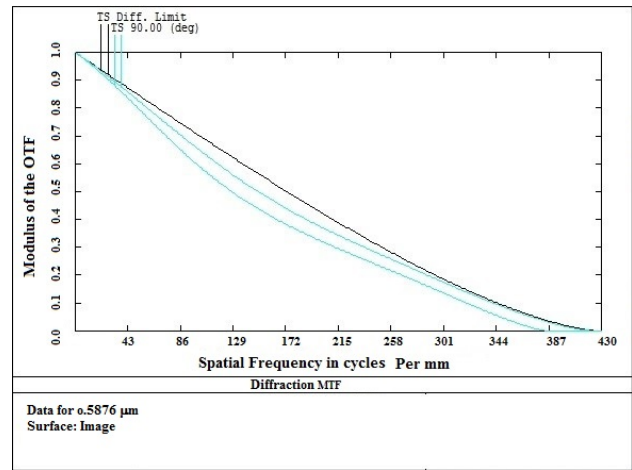


Figure 10. MTF diagram at -46 °C temperature at 90° field angle in wavelength of d.

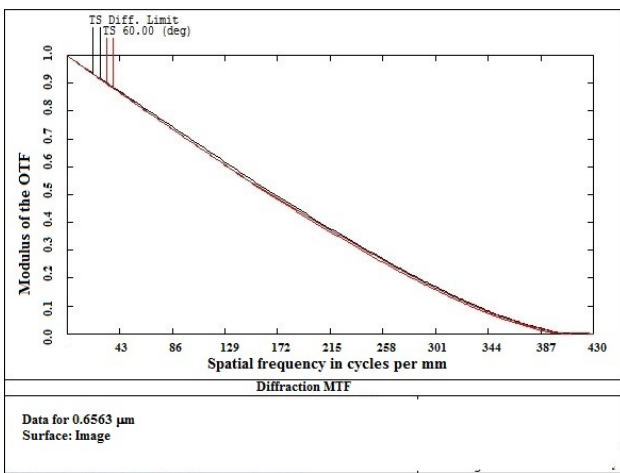


Figure 9. MTF diagram at 70 °C temperature at 60° field angle in wavelength of C.

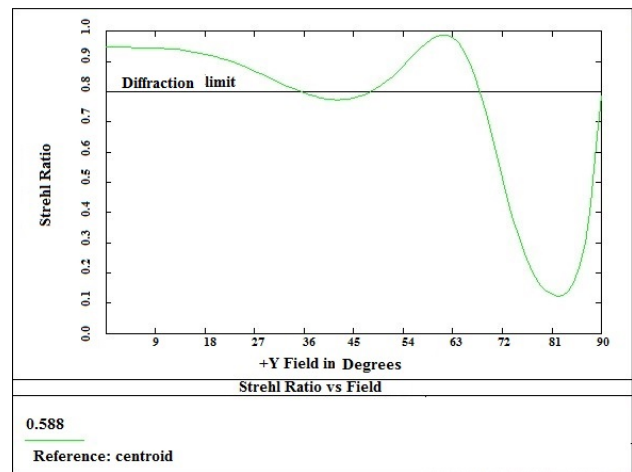


Figure 11. Strehl ratio diagram versus half field of view at -46 °C temperature in the central wavelength (spectral line d).

gram. If an optical system is ideal and without aberrations, its MTF diagram is tangent to this diagram [25]. The MTF diagram for the tangential rays *T* (meaning the rays placed in the vertical plane) and the sagittal rays *S* (meaning the rays placed in the horizontal plane) are drawn separately. In this diagram, the *x*-axis is the spatial frequency in units of line pairs per millimeter, and the *y*-axis is the absolute value of the phase transfer function (contrast). A human generally needs a contrast of 0.1 or higher to be able to see the difference between lines. The black curve is the diffraction limit diagram. If an optical system is ideal and without aberrations, its MTF diagram is tangent to this diagram [25]. The MTF diagram for the tangential rays *T* (meaning the rays placed in the vertical plane) and the sagittal rays *S* (meaning the rays placed in the horizontal plane) are drawn separate. Figures 7 to 10 show that the MTF diagrams are close to their diffraction limit curve, which indicates the correction of the aberrations of the athermalized fisheye system.

Figures 11 and 12 show the Strehl ratio diagram in terms of the lower half field of view from zero to 90 degrees for the central wavelength i.e. spectral line d at -46 and 70

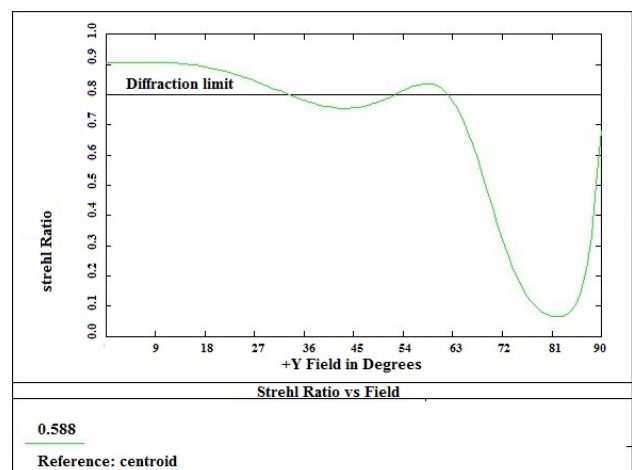


Figure 12. Strehl ratio diagram versus half field of view at 70 °C temperature in the central wavelength (spectral line d).

degrees Celsius, respectively.

The Strehl ratio is defined as the ratio of the central intensity an aberrated image of an object point to the central intensity in the unaberrated pattern. Due to phenomenon diffraction, even a focusing system that is perfect according to geometrical optics will have a limited spatial resolution. In the usual case of a uniform circular aperture, the point spread function (PSF) which describes the image formed from a point source is given by the Airy disc. For a circular aperture, the peak intensity at the center of the Airy disc defines the point source image intensity required for unit Strehl ratio. A non-ideal optical system using the same physical aperture will generally produce a wider PSF where the peak intensity is reduced by a factor given by the Strehl ratio [26]. An optical system with only minor imperfections in this respect may be referred to as "diffraction limited" because its PSF closely resembles an Airy disc. A Strehl ratio greater than 0.8 is often cited as a criterion for using that name. It can be seen in Figures 11 and 12 that the Strehl ratio for half the field of view from zero to about 70 degrees is close to the diffraction limit, which indicates the excellent optical performance of the system. At an angle higher than 70 degrees, the Strehl number decreases significantly, the main factor of which is distortion aberration at angles close to 90 degrees. At the angles of the large field, close to 90 degrees, the height of the image increases a lot, and in order for the entire image to fit in the image plane, it is necessary to create a distortion aberration. Therefore, distortion is an inseparable aberration of the fish-eye lens, and in order for the image to fit in the two half-angles of the field zero to 90 and -90 to zero in the image plane, we must have distortion. But it should be noted that the quality of the image does not decrease in distortion, but the shape of the image changes. That is, the image of the object point in the paraaxial plane is slightly shifted compared to when there is no path.

4. Conclusion

In this work, a type of fisheye optical system was redesigned in the visible spectral region with a field of view of 180 degrees and then athermalized for Iran's temperature conditions from -46 to 70 degrees Celsius. The fish-eye lens is a bionic system that mimics the eyes of underwater fish looking at the upper half of the world. A fish immersed in water places its eyes directly on the surface of the water and sees objects above the surface as a compressed circular image with a field of view of approximately 180 degrees, although the image is strongly distorted at the edge. The redesigned system in this work includes a front lens group and a rear lens group. The front group includes 5 lenses with negative total power and the rear group includes 9 lenses with positive total power. The parameters that determine the quality of the image such as spot diagram, modulation transfer function and Strehl ratio showed that the system is well athermalized in the temperature range of Iran in the wavelengths of the visible region. For example, the RMS radius of the spot diagram for Iran's temperature range from -46 to 70 degrees Celsius in the half field of view from zero to about 70 degrees (also the half field of view from -70 to

zero degrees) in the central wavelength of the visible light is smaller than the diffraction limit radius of the Airy disc. At most angles greater than 70 degrees (except for a few) the RMS radius becomes larger than the radius of the Airy disc, which is the reason for the existence of distortion and that is impossible to eliminate at the edges of the image. Because in order for the entire image from the field of view of zero to 180 degrees to fit in the image plane, the image must be distorted. Distortion aberration does not reduce the contrast and clarity of the image, but change the shape of the image. Another work that can be done on this system is the design of the achromat athermalization fisheye system in Iran's temperature range to correct color aberrations, which is suggested to researchers and specialists in this field.

Authors Contributions

All the authors have participated sufficiently in the intellectual content, conception and design of this work or the analysis and interpretation of the data (when applicable), as well as the writing of the manuscript.

Availability of Data and Materials

The data that support the findings of this study are available from the corresponding author upon reasonable request.

Conflict of Interests

The authors declare that they have no known competing financial interests or personal relationships that could have appeared to influence the work reported in this paper.

Open Access

This article is licensed under a Creative Commons Attribution 4.0 International License, which permits use, sharing, adaptation, distribution and reproduction in any medium or format, as long as you give appropriate credit to the original author(s) and the source, provide a link to the Creative Commons license, and indicate if changes were made. The images or other third party material in this article are included in the article's Creative Commons license, unless indicated otherwise in a credit line to the material. If material is not included in the article's Creative Commons license and your intended use is not permitted by statutory regulation or exceeds the permitted use, you will need to obtain permission directly from the OICC Press publisher. To view a copy of this license, visit <https://creativecommons.org/licenses/by/4.0>.

References

- [1] J. Wang and C. Xue. "Athermalization and thermal characteristics of multilayer diffractive optical elements.". *Applied Optics*, **54**:9665–9670, 2015. DOI: <https://doi.org/10.1364/AO.54.009665>.

- [2] H. Xie, Y. Su, M. Zhu, L. Yang, S. Wang, X. Wang, and T. Yang. "Athermalization of infrared optical system through wavefront coding.". *Optics Communications*, **441**:106–112, 2019. DOI: <https://doi.org/10.1016/j.optcom.2019.02.043>.
- [3] K. Schwertz, D. Dillon, and S. Sparrold. "Graphically selecting optical components and housing material for color correction and passive athermalization.". *Current Developments in Lens Design and Optical Engineering XIII*, **8486**:110–127, 2012. DOI: <https://doi.org/10.1117/12.930968>.
- [4] S. N. Kasarova, N. G. Sultanova, and I. D. Nikolov. "Temperature dependence of refractive characteristics of optical plastics.". *Journal of Physics: Conference Series, IOP*, **253**:1261–1266, 2010. DOI: <https://doi.org/10.1088/1742-6596/253/1/012028>.
- [5] C. Sahin. "The geometry and usage of the supplementary fisheye lenses in smartphones.". *Smartphones from an Applied Research Perspective*, , 2017. DOI: <https://doi.org/10.5772/intechopen.69691>.
- [6] C. Hughes, P. Denny, E. Jones, and M. Glavin. "Accuracy of fish-eye lens models.". *Applied optics*, **49**:3338–3347, 2010. DOI: <https://doi.org/10.1364/AO.49.003338>.
- [7] R. Hill. "A lens for whole sky photographs.". *Quarterly Journal of the Royal Meteorological Society*, **50**:227–235, 1924. DOI: <https://doi.org/10.1002/qj.49705021110>.
- [8] R. W. Wood. "Fish-eye views, and vision under water.". *The London, Edinburgh & Dublin Philosophical Magazine and Journal of Science*, **12**:159–162, 1906. DOI: <https://doi.org/10.1080/14786440609463529>.
- [9] K. Miyamoto. "Fish eye lens.". *Journal of the Optical Society of America*, **54**:1060–1061, 1964. DOI: <https://doi.org/10.1364/JOSA.54.001060>.
- [10] C. B. Martin. "Design issues of a hyper-field fisheye lens.". *Novel Optical Systems Design and Optimization VII. SPIE*, , 2004. DOI: <https://doi.org/10.1117/12.563190>.
- [11] W. N. Bond. "A wide angle lens for cloud recording.". *Philosophical Magazine Series 6*, **44**:999–1001, 1922. DOI: <https://doi.org/10.1080/14786441208562576>.
- [12] H. Guozhu and L. Lijun. "Design of zoom fish-eye lens systems.". *Infrared and Laser Engineering*, **49**:20190519–1–10, 2020. DOI: <https://doi.org/10.3788/IRLA20190519>.
- [13] M. Laikin. "Lens design, 4th Edition.". *CRC Press*, , 2006. DOI: <https://doi.org/10.1201/9780849382796>.
- [14] R. Kingslake and R. B. Johnson. "Lens design fundamentals, 2th Edition.". *Academic Press*, , 2009. DOI: <https://doi.org/10.1016/B978-0-12-374301-5.00005-X>.
- [15] C. H. F. Velzel. "A course in lens design.". *Springer*, , 2014. DOI: <https://doi.org/10.1007/978-94-017-8685-0>.
- [16] Y. Yan and J. Sasian. "Photographic zoom fish-eye lens design for DSLR cameras. ". *Optical Engineering*, **56**:095103–095103, 2017. DOI: <https://doi.org/10.1117/1.OE.56.9.095103>.
- [17] H. Kim, J. Jung, and J. Paik. "Fisheye lens camera based surveillance system for wide field of view monitoring.". *Optik*, **127**:5636–5645, 2016. DOI: <https://doi.org/10.1016/j.jlleo.2016.03.069>.
- [18] A. Rezaei-Latifi. "Design of a three-element apochromatic lens to correct axial chromatic aberration at UVA wavelength band.". *Journal of Optoelectrical Nanostructures*, **8**:63–81, 2023. DOI: <https://doi.org/10.30495/JOPN.2024.31998.1291>.
- [19] J. Sasián. "Introduction to lens design.". *Cambridge University Press*, , 2019. DOI: <https://doi.org/10.1017/9781108625388>.
- [20] T. H. Jamieson. "Thermal effects in optical systems.". *Optical Engineering*, **20**:156–160, 1981. DOI: <https://doi.org/10.1117/12.7972683>.
- [21] X. Q. Ai, B. Liu, X. Zhang, and H. Jia. "Thermal difference analysis and athermalization design of infrared optical system..". *Optical Design and Testing IV*, **7849**, 2010. DOI: <https://doi.org/10.1117/12.869543>.
- [22] T. Huber, H. P. Degischer, G. Lefranc, and T. Schmitt. "Thermal expansion studies on aluminium-matrix composites with different reinforcement architecture of SiC particles.". *Composites Science and Technology*, **66**:2206–2217, 2006. DOI: <https://doi.org/10.1016/j.compscitech.2005.12.012>.
- [23] P. Alamdari, O. Nematollahi, and A. A. Alemrajabi. "Solar energy potentials in Iran: A review. ". *Renewable and Sustainable Energy Reviews*, **21**:778–788, 2013. DOI: <https://doi.org/10.1016/j.rser.2012.12.052>.
- [24] G. Fallah-Ghahhari, F. Shakeri, and A. Dadashi-Roudbari. "Impacts of climate changes on the maximum and minimum temperature in Iran.". *Theoretical and Applied Climatology*, **138**:1539–1562, 2019. DOI: <https://doi.org/10.1007/s00704-019-02906-9>.
- [25] A. Rezaei-Latifi. "Design of a type of optimal optical spectrometer in the UV-A spectral region. ". *Journal of Applied Electromagnetic*, **2**:1–8, 2023. DOI: <https://doi.org/10.1001.1.26455153.1402.11.2.12>.
- [26] V. N. Mahajan. "Strehl ratio for primary aberrations in terms of their aberration variance.". *JOSA*, **73**:860–861, 1983. DOI: <https://doi.org/10.1364/JOSA.73.000860>.